https://doi.org/10.3311/PPci.41236

Periodica Polytechnica Civil Engineering

Impact of Environmental Pressure Changes on High Precision Measurements

György Szondy[1*]

[1] Department of Geodesy and Surveying, Faculty of Civil Engineering, Budapest University of Technology and Economics, Műegyetem rkp. 3., H-1111 Budapest, Hungary
[*] Corresponding author, e-mail: szondy.gyorgy@emk.bme.hu

Received: 10 June 2025, Accepted: 08 January 2026, Published online: 02 February 2026

Abstract

Stable environmental temperature is essential for high precision measurements. Underground caves, or underground laboratories, far from the entrance are generally assumed to provide such ideal, extremely stable environment. However, atmospheric pressure variations have an indirect effect on the temperature of such sites. Two relevant effects are adiabatic temperature change and pressure-dependent self-heating of electronic instruments. In this study a 64-days long temperature timeseries recorded by a tilt-meter was analysed to identify and characterize these effects. We found that large, slow temperature changes can be removed properly, allowing both of the aforementioned effects to be detected in the residual. Furthermore, some key parameters of the pressure–temperature transfer function can be estimated. However, a precise model of pressure dependence could not be obtained, possibly due to the nonlinear behaviour of the process and/or insufficient excitation levels. The results demonstrate that these two effects impose opposite requirements on the instrument's thermal insulation of the instrument. Consequently, either these effects should be taken into consideration, or the generated heat should be conducted away through a properly sized metallic path eliminating the pressure dependence of self-heating.

Keywords

high-precision measurement, adiabatic temperature change, self-heating, tilt meter, underground laboratory, relaxation, quantization principle

1 Introduction

The basic assumption of Einstein's theory of General Relativity is the equivalence of gravitational and inertial mass (that is, that the gravitational acceleration of bodies does not depend on the quality of matter). If so, then the gravitational force can be regarded as an inertia force, so that the gravitational field can be replaced by an accelerating coordinate system. Einstein relied primarily on the results of the Eötvös-Pekár-Fekete, also known as EPF experiment, carried out by the Hungarian physicist Loránd Eötvös with two of his colleagues, Dezső Pekár and Jenő Fekete, between 1906 and 1908. The experiment confirmed the equivalence of the gravitational and inertial mass with 10^{-8} precision, 3 orders of magnitude more precisely than before [1].

However, in 1986, Ephraim Fischbach and his team found that some 10^{-9} variations in the measurement, which were previously thought to be random, correlate with the binding energy of the nuclei of the materials of test masses used for the experiment [2]. The discovery caused huge excitement, especially because it contradicted recent experiments [3, 4] carried out till then, therefore Fischbach and his team suspected the existence of a new short-range "fifth force". However, the existence of this new force has not been confirmed and has been dismissed by the scientific community. A recent hypothesis concerning the discrepancies is related to Gyula Tóth, who explains the effect by the different shape causing different coupling factor of the test masses [5].

To commemorate the 100th anniversary of Eötvös' death and to honour his work, in association with the HUN-REN Wigner Research Centre for Physics (Wigner RCP) and the Department of Geodesy and Surveying of Budapest University of Technology and Economics (BME) we started to repeat the EPF experiment [6–8]. We intended to perform the experiment by upgrading a 1930 Pekár Eötvös torsion balance using

Cite this article as: Szondy, G. "Impact of Environmental Pressure Changes on High Precision Measurements", Periodica Polytechnica Civil Engineering, 2026. https://doi.org/10.3311/PPci.41236

modern measurement techniques. The measurement was carried out at a depth of 30 m in a laboratory of the Jánossy Underground Research Laboratory (JURLab) unit of the Vesztergombi Laboratory of High Energy Physics (VLAB) at Wigner Research Centre for Physics.

The Eötvös torsion-balance is designed to measure most of the second derivatives of the gravitational potential. The measurement is performed in 4 different azimuths per iteration. To measure one azimuth takes 1 to 2 h, depending on the damping of the pendulum's oscillation. In order to achieve sufficient accuracy and to filter out external disturbances, a complete measurement cycle consists of 50 to 100 iterations, which means 1 to 2 weeks continuous operation per measurement cycle.

Earlier modernization efforts [9] solved automatic readout with 1 s sampling time while our current development achieved 2-3 orders better resolution than the readout of Eötvös. We solved the automatic rotation and precise readout of the azimuth as well as supporting the unsupervised execution of several weeks long measurement cycles [6].

Preliminary measurements have shown that, with the increased sensitivity, environmental disturbances, in particular pressure and temperature changes, as well as the effects of natural and artificial microseismical noise, can now be detected [10]. It became also obvious, that these disturbances are preventing us achieving the desired accuracy. Therefore, we started to investigate the mechanism of environmental disturbances and the possibility of their compensation.

One such effect under investigation is the effect of pressure changes on the signal measured by the torsion-balance through temperature changes and the tilt caused by environmental deformation.

The other important perturbation is the temperature effect of laboratory lighting due to human presence. Switching on the lamps causes indirect error signal through temperature orders of magnitude larger than the signal to be measured. However, in case of tiltmeters, due to its small size, this transient thermal effect can be reduced by orders of magnitude by using thermal insulation cover.

The Jánossy underground laboratory 30 m below ground level, behind two closed doors, provides thermal conditions similar to deep caves. At first glance, one might think that – if there is no human disturbance – underground caves, far from the entrance, provide an extremely stable environment in terms of temperature [11]. However, as confirmed by previous studies by Perrier et al. [11, 12], and as we have experienced earlier using our thermometer with a relatively poor resolution of 10 mK in such places a sudden change of pressure can cause an adiabatic temperature change (Fig. 1).

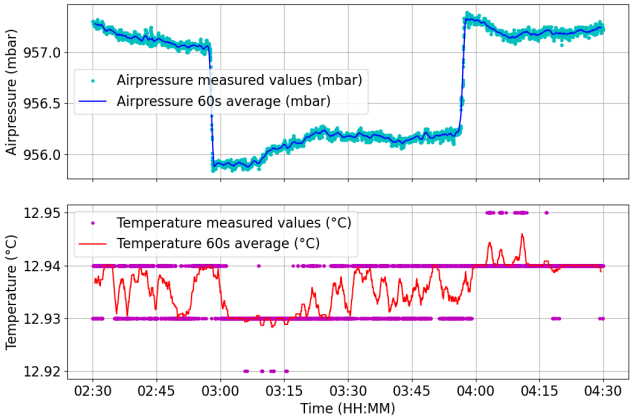

Fig. 1 A pressure jump of 1mbar in the laboratory (upper diagram), resulted a temperature change of a few mK (lower diagram) that can even be detected using a 10 mK resolution thermometer. Individual measurements are indicated by dots (light blue and magenta), while solid lines are 60 s averaged values (dark blue and red).

In addition, this temperature stability was lost in the summer of 2024, due to a technical failure (pipe break) and the subsequent drying of the lab. When the measurement was restarted the temperature of the laboratory – due to this intervention – was several degrees higher, and it took several months to return to the normal, equilibrium temperature.

However, this non-ideal situation highlighted two important aspects of measurements. The first is that the quantization error in temperature measurement and especially the neglect of quantization principles [13] causes systematic error and clearly determine the achievable resolution as well as the relative error of the measurement.

The second is that natural, well-modelled transient (relaxation) processes can be removed from the measurement data by appropriate curve-fitting, allowing the investigation of processes and effects in the residual with amplitudes 2-3 or even more orders of magnitude smaller than the disturbing transient process.

In our case, there are at least two observable effects in the temperature residual. One is the adiabatic temperature change that occurs in case of significant, rapid pressure changes (see Fig. 2).

The other effect, however, becomes obvious when looking the whole time series, i.e. that the temperature residual is anticorrelated with atmospheric pressure with a delay of a few hours (Fig. 3). Looking at the thermal processes, this is related to the so-called self-heating effect, where the electronics of the instrument produce heat while cooling through the air. Under the thermal insulation, as the cooling surface (floor area) is smaller, the thermal coupling is worse, causing larger self-heating effect. With air pressure changes, the thermal coupling, cooling of the instrument, and thus the self-heating effect also changes. This

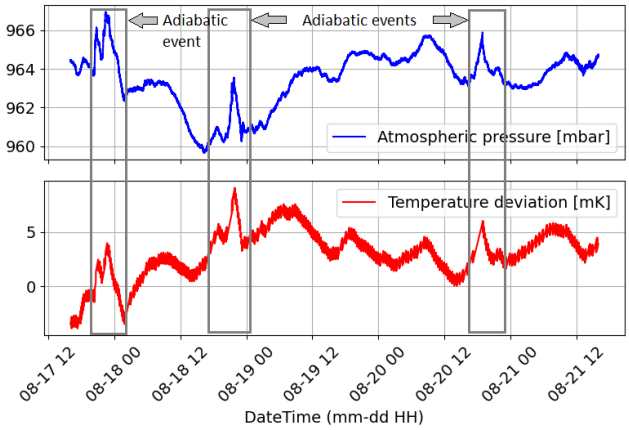

Fig. 2 Rapid pressure changes (blue curve) and adiabatic temperature changes (red curve) in the Jánossy Underground Laboratory during the 60+ days observation period between August 2024 and October 2024.

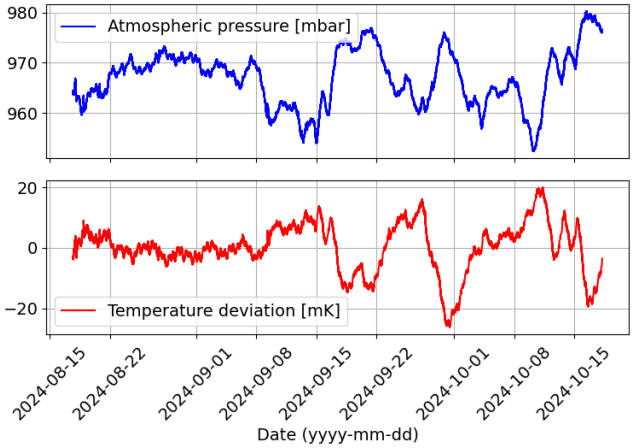

Fig. 3 Diagram of the pressure (blue curve) and temperature residual (red curve) over the 60+ day observation period between August 2024 and October 2024 in the Jánossy Underground Laboratory. The two diagram shows that temperature residual is clearly anticorrelated with atmospheric pressure with some delay.

self-heating effect has previously been studied by Babita and others mainly for thermometers, where it was found to be a few mKs and with calibration it could be corrected with an uncertainty of 20 μK [14]. It is also well known that neither heat radiation nor heat conduction is not temperature dependent at normal atmospheric pressure [15], so the change is clearly due to the pressure dependence of the thermal coupling by a convective flow [16].

2 Location, equipment and methods

2.1 The Jánossy underground laboratory

The Jánossy underground laboratory is located in Budapest, on the premises of the HUN-REN Wigner Research Centre for Physics, 6.4 km west of the city centre, in the Buda Hills, about 700-1200 m from residential areas (Fig. 4) [17]. Within the site, the laboratory itself is located on a sloping area 30 m below the surface, 50–200 m from other buildings in use.

The Jánossy underground laboratory complex consists of a 30 m deep vertical pit and horizontal tunnel-like tunnels of varying lengths, 2.5 m high and 2.5 m wide, opening in different directions at −10, −20 and −30 m (Fig. 5). The surrounding soil is a mixture of sedimentary limestone and clay. The walls of the laboratory are whitewashed, cladding and insulation-free, high-strength reactor concrete. Although the external entrance is closed by a heavy iron door, as used in shelters, the closure is not airtight. Upon entering the facility, one reaches a vertical shaft. In the centre, there is an elevator, while a spiral staircase winds around it, leading down to the lower levels. There are laboratories at 10, 20, and 30 meters deep. Each laboratory is separated from the vertical shaft by a brick wall and a standard-sized door.

Our laboratory is located at level −3 (30 m deep), and is a 20 m long tunnel pathway at an angle of −7° to the north.

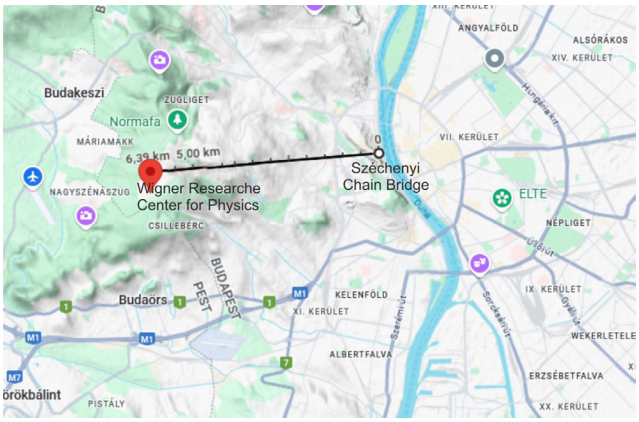

Fig. 4 The underground lab is located on the site of the Wigner Research Centre for Physics, ~6.4 km from the centre of Budapest and ~1 km from residential areas [17]

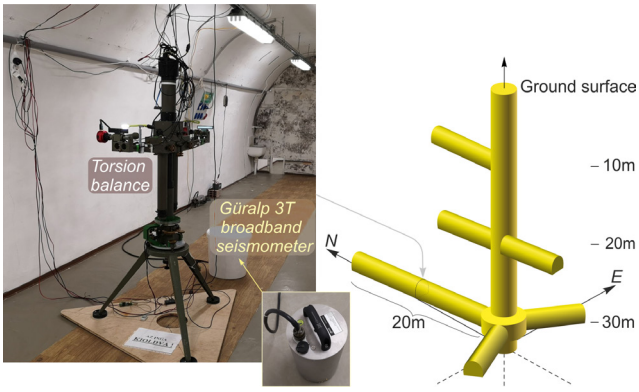

Fig. 5 Sketch of the Jánossy Underground Laboratory and the location of the Eötvös torsion-balance (Copyright © Lajos Völgyesi et al. [10])

The torsion balance, its associated digital thermometer and the Lippmann high resolution Tiltmeter (LTS) are located approximately in the geometric centre of the tunnel, equidistant from the walls.

Air circulation is basically provided by a programmable air-conditioning system. The temperature of the laboratory is generally stable, around 12–12.5 °C all year round, unless it needs to be heated for some reason, or if the laboratory lighting or some electrical equipment of considerable power is operated for a longer period. The relative humidity, especially in summer, usually rises slowly to over 90%. For this reason, it is necessary to dehumidify the laboratory every few weeks, using commercially available dehumidification equipment.

However, considering that dehumidification and air-conditioning have significant noise and thermal effect, we did not use them during the observation period.

2.2 Instrumentation, instrument placement, data series

A large part of the laboratory data collection and measurement control (laboratory temperature, pressure, humidity, pendulum scale reading and control, camera-based motion detection, data archiving) is performed by a data acquisition computer located on the carousel in front of the laboratory. As the door to the lab is permanently closed, the heat from this machine is not felt in the lab. The electronics inside the lab are ZWO ASI 224 MC and 385 MC astronomical cameras (P < 1 W), ESP32 based data acquisition and measurement control modules (P < 100 mW), a Lippmann high resolution Tiltmeter (LTS) (12 V/20 mA < 240 mW) [18], its battery charger at the lab entrance (P = 0.3–1W, typically 0.5 W) and the Raspberry Pi 4 computer for data collection (P = 2.5–5 W), as well as a Güralp 3T seismometer (P = 0.75 W).

During the present measurement, only the Lippmann Precision Tiltmeter (LTS), its charger and data logger were in continuous operation. The Güralp 3T seismometer was started up in the last two weeks of the measurement period, just before 17:30 on 02.10.2024.

The Lippmann Tiltmeter (LTS) was set up in the centre of the lab, where the Eötvös torsion balance (ETB) is located. A 0.8 m wide PVC strip runs along the entire length of the lab, in the middle, and was removed from an area of 0.04 m^2 under the ETB. Here, an iron instrument platform equipped with levelling screws was set up for the LTS. To eliminate transient temperature effects on the tiltmeter, we used a 100 mm thick Styrofoam thermal insulation with internal dimensions of 0.9 m × 0.4 m × 0.5 m (l/w/h) (Fig. 6) following the setup applied by Meurers et al. [19] and Barbély et al. [20],

LTS itself measures pressure, temperature and relative humidity with a resolution of 1 Pa, 1 mK and 0.01%, and X/Y tilt with resolution of nano radian ($2 \cdot 10^{-4}$ arcsecs). The housing of the LTS is 100 mm × 80 mm × 120 mm (l/w/h) painted aluminium with a 9 pin RS232 connector for communication. The particular instrument used for the measurement is almost completely air-tight, which means that the internal pressure of the instrument follows the change of the external air pressure only with a delay of several hours, but immediately the rise due to the change of external temperature (Fig. 7).

The LTS data (X-tilt, Y-tilt, temp, humidity, air pressure) were recorded at 1 second resolution by a Raspberry PI 4 computer placed outside the thermal insulation at a distance of ~0.4 m. It was connected to the network of the

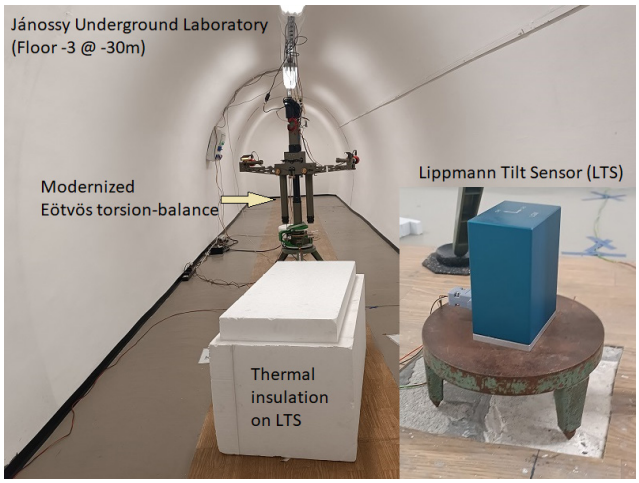

Fig. 6 The Lippmann precision tiltmeter (LTS), with the instrument stand used (bottom right) and the Styrofoam insulation cover (centre)

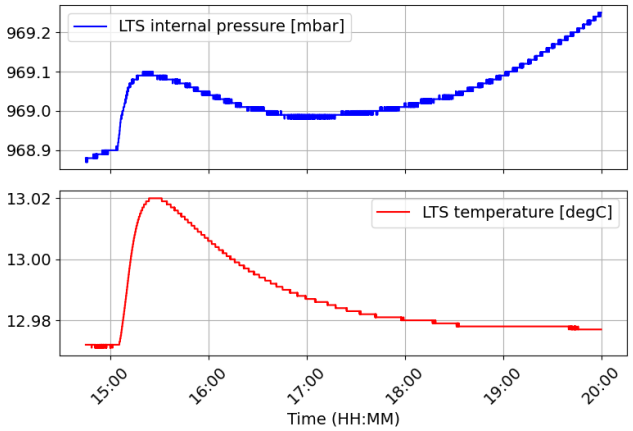

Fig. 7 The internal pressure of the LTS instrument (upper curve) slowly increases (~0.1 mbar/h) due to the external pressure change while dynamically follows the change in external temperature (lower curve).

research institute via UTP. Network connection is used for Network Time Protocol (NTP) time synchronization and accessing the collected data.

To measure atmospheric pressure outside LTS, we used BMP280 sensor and a custom-built ESP32 based data logger. The instrument was placed outside in the lobby of the Jánossy laboratory, above the external iron door. The data logger was connected via WiFi to the IoT network of the research centre and used NTP service to secure the time-stamp for data collection. The temperature and pressure data were stored on a built-in SD card with a sampling rate of 1 s and a resolution of 0.01 K and 0.01 Pa, respectively.

As the external air pressure was measured at the main entrance, 30 m above the laboratory, the actual pressure in the lab was approximately 40 Pa higher and a few seconds delayed relative to the measured value. However, since the processes under investigation evolved over much larger timescales, for the present experiment this small delay was considered negligible.

2.3 Fitting the cooling curve to the temperature

At the beginning of the measurement period, the temperature in the lab was 15.1 °C, more than one and a half degrees higher than the equilibrium. Consequently, the temperature during the measurement period was approaching the equilibrium. In previous experiments we found that in such cases, after appropriate curve fitting, the residual is suitable for observing other, much smaller effects, therefore we searched for a suitable model and determined its parameters (Fig. 8).

As a first hypothesis, we assumed that the cooling curve was an exponential function, but since this did not give a satisfactory approximation, we added more terms, like a linear, a quadratic, a second and a third exponential. Then

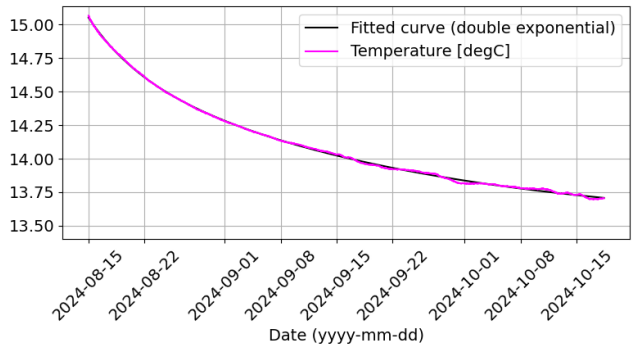

Fig. 8 The laboratory temperature (magenta) and the fitted cooling curve (black). The cooling process over more than two months was fitted by a sum of two exponential terms, reproducing the data within ± 20mK.

we executed the fit function using different combinations of the terms. See all the terms in Eq. (1):

$$\hat{T} = T_0 + \Delta T_1 e^{-\frac{t}{\tau_1}} + \Delta T_2 e^{-\frac{t}{\tau_2}} + \ldots + a_1 t + a_2 t^2 \,. \tag{1}$$

The results of the modelling showed that even the exponential with the linear term did not give a good approximation, neither qualitatively (see Fig. 9) nor quantitatively (see Table 1), while the differences between the results of more complex models were not significant.

Considering that the two exponential model described by Eq. (2) was the one that can be explained physically, i.e. the solution of second order linear homogeneous differential equation, we used this approximation in the further analysis.

$$\hat{T} = T_0 + \Delta T_1 e^{-\frac{t}{\tau_1}} + \Delta T_2 e^{-\frac{t}{\tau_2}} \tag{2}$$

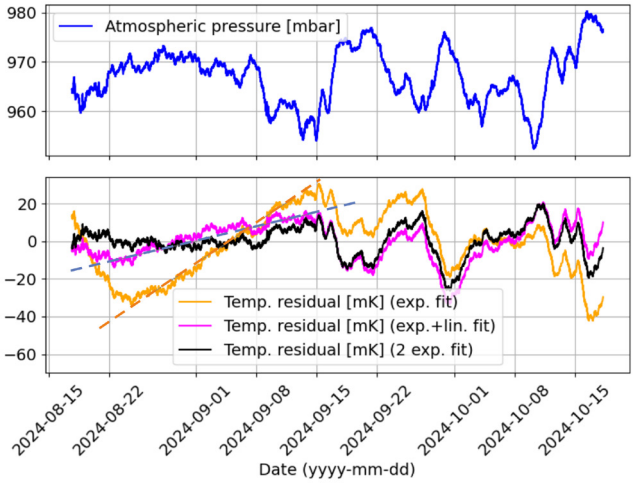

Fig. 9 Pressure curve (upper diagram) and some of the temperature residuals (lower diagram) that were obtained using different mathematical models: exponential (yellow), exponential with linear trend (magenta) and two exponentials (black). The first two seems to have an unexplainable linear tendency during the first half of the period.

Table 1 The standard deviation of the residuals with different fit functions.

Name of the function	Fit-function	σ [K]
ExpFitFunction	1 exponential	0.0200
ExpLinFitFunction	1 exponential + linear	0.0106
ExpQuadFitFunction	1 exponential + quadratic	0.0081
DoubleExpFitFunction	2 exponentials	0.0080
DoubleExpLinFitFunction	2 exponentials + linear	0.0080
DoubleExpQuadFitFunction	2 exponentials + quadratic	failed
TripleExpFitFunction	3 exponentials	0.0080

The parameters obtained from a least square fitting procedure are presented in Eq. (3), where temperature parameters are in °C and time constants are in days.

$$\hat{T} = 13.490 + 1.218e^{-\frac{t}{37.35}} + 0.343e^{-\frac{t}{5.98}} \quad (3)$$

According to the parameters, the temperature was initially 1.561 °C higher than the equilibrium. The cool down process had time constants of 5.98 and 37.35 days. This kind of model (the sum of exponentially decaying modes) is usual in heat-diffusion processes [21], especially in case of multi-layered environment [22]. However, modelling of the heat transfer between the air, the concrete walls and the surrounding soil is beyond the scope of the present study. After the 64 days cool down period temperature still not reached its equilibrium state. The remaining difference was still approximately +0.22 °C.

2.4 Qualitative analysis of the temperature residual

After the fitted cooling curve is subtracted, two relationships can be seen at first glance by comparing the temperature residual with the atmospheric pressure. The first one is the anticorrelation of temperature with pressure can be read from the figure for the whole measurement period. The other effect that can be found by zooming in on individual periods is the expected instantaneous adiabatic temperature change, previously studied by Perrier et al. [11, 12].

As outlined in the introduction, the delayed anticorrelation arises from the interaction between the instrument's self-heating and its cooling processes. The instrument's natural convection–based cooling depends on atmospheric pressure: higher pressure results in more efficient cooling. Consequently, the equilibrium temperature of the instrument will also be pressure-dependent. Upon a pressure change, the instrument's temperature approaches the new equilibrium state with a characteristic time constant. If temperature is measured with sufficient precision, and both the pressure dependency of the self-heating or equilibrium temperature and the corresponding time constant are determined, the effect of these slow processes can be compensated.

Since in the long-term self-heating effect clearly dominates the temperature change of the instrument, adiabatic events can be detected only in case of rapid pressure changes. The simplest way to identify such events is by examining the time derivative of pressure (Fig. 10).

One can expect a third effect as well, namely that cooler outside air leaks inside the cover during a pressure

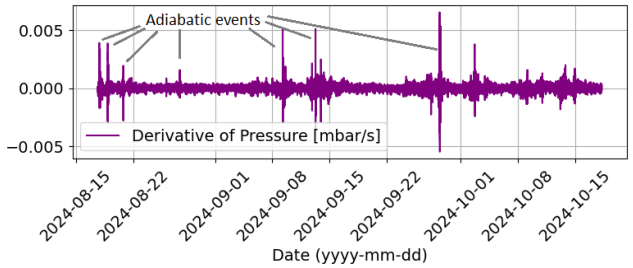

Fig. 10 The pressure derivative shows clearly identifiable adiabatic events (peaks)

increase, cooling the internal air. Although this instantaneous effect is similar to the adiabatic change, it is significantly smaller in magnitude. From $dT_{\text{leaking}} \sim \Delta T \cdot dp/p$ and $dT_{\text{adiabatic}} \sim 2/7 \cdot T \cdot dp/p$, and since $2/7 \cdot T$ typically exceeds ΔT by about two orders of magnitude, the adiabatic change dominates, therefore the cooling effect due to the air leakage would be difficult to identify.

To investigate further the adiabatic effect, 3 such approximately 4 days long periods ($1/16^{\text{th}}$ of the whole observation) were selected (Figs. 2 and 11).

2.5 Preparing and correcting temperature data

Unfortunately, the temperature residual was subject to systematic error due to quantization, which was largely corrected by the subtracted cooling curve, but the temperature residual still included a sawtooth signal, whose frequency

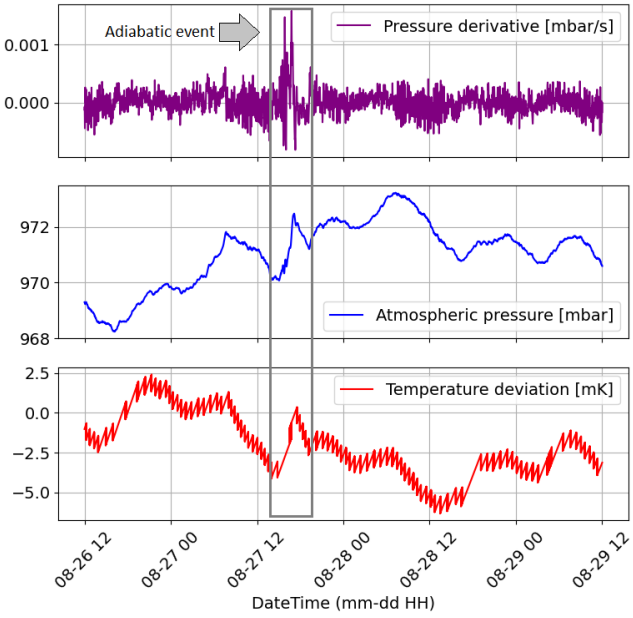

Fig. 11 Events identified from the pressure time derivative (upper, purple panel) coincide with sudden pressure change (middle, blue diagram) that causes immediate, in-phase, adiabatic temperature response (lower, red curve). Meanwhile the temperature diagram clearly shows a 1mK peak-to-peak sawtooth like noise.

depends on the slope of the temperature change. The amplitude and high frequency component of the sawtooth prevents us determining the precise temperature and the transfer function in the frequency range of the error. To cope with the issue of precision the temperature signal had to be filtered/smoothed such a way that the smoothed curve approximated the actual residual value as good as possible.

Smoothing was done by resampling the temperature residual in reference points where the precision is high, and fitting a second-degree curve on these points. Reference point selection is based on the assumption that temperature values are the most accurate at the change of measured value and the best approximation is the mean of the upper and lower value of the step. However, changes of the measured temperature values were not instantaneous.

It usually changes from one level to another after some fluctuation. Therefore, we grouped the back-and-forth oscillations belonging to the same two levels with a time-gap smaller than 5 min and used the average timestamp and average value of the grouped changes as reference points (Fig. 12). Because the reference points are irregularly spaced, there is no single Nyquist frequency. Using the shortest interval (5.4 min) a theoretical upper limit is $1.5 \cdot 10^{-3}$ Hz ($t_{\text{period}} > 0.2$ h). Using the median interval from 31 min (1st quarter) to 51 min (2-4th quarter) gives a typical bound around $2.7 \cdot 10^{-4}$ Hz and $1.6 \cdot 10^{-4}$ Hz. In practice the maximum sampling interval (~7 h 40 min) indicates that the effective cutoff frequency of the resampled data might be closer to 1/(12 h) ≈ $2.3 \cdot 10^{-5}$ Hz. We also estimated the uncertainty of the temperature values at the reference points from the rate of transition time and sampling time and found it to be less than ±0.03 mK. It means, that the accuracy of the measurement at these certain points has been significantly increased.

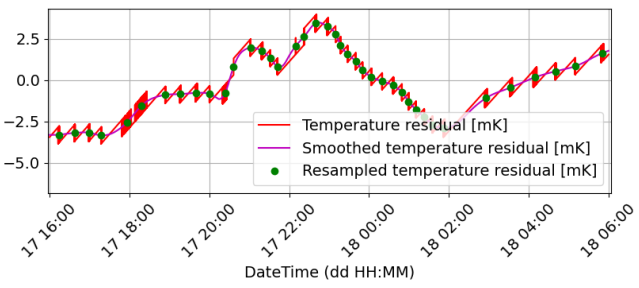

Fig. 12 Smoothed curve (magenta) of the temperature residual (red) built on the selected resampling points (green). The time distance between samples is uneven, varies from 5.4 min to several hours depending on the temperature changes and the actual slope of the original temperature curve.

2.6 Determine the delay of self-heating

From the pressure–temperature residual diagram it was obvious that temperature was anticorrelated with pressure, with a delay of several hours. The delay was estimated from the cross-correlation of the two signals by dividing the full time series into 16 segments of equal length and determining the position of the maximum of the cross-correlation for each segment. In one of them the delay time could not be determined, while in two other cases outlier values were obtained. These erroneous estimates occurred when a substantial pressure change (15–20 mbar) took place within a short period of time. Based on the remaining 13 segments, the delay of the temperature variation relative to the pressure was found to be 5.21 ± 0.7 h at the 95% confidence level.

2.7 Determine the pressure-temperature transfer function

To determine the pressure-temperature transfer function, we decided to apply the robust method used by Pierre et al. [11], where the entire time series is cut into N separate pieces and the transfer function is calculated from these according to the following general formula in Eq. (4):

$$G_{a,b}^{c}\left(f_j\right) = \frac{\sum_{k=0}^{N-1} \hat{a}_{j,k}\,\overline{\hat{c}_{j,k}}}{\sum_{k=0}^{N-1} \hat{b}_{j,k}\,\overline{\hat{c}_{j,k}}}, \tag{4}$$

where $G_{a,b}^{c}$ is the transfer function, a is the dependent variable (in our case T), b is the independent variable (in our case p) and c is the reference variable (p in or case), f_j is the j^{th} frequency, $\hat{a}_{j,k}$, $\hat{b}_{j,k}$ and $\hat{c}_{j,k}$ are the complex discrete Fourier transform of the k^{th} piece of the time series a, b and c respectively at the j^{th} frequency and $\overline{\hat{c}_{J,k}}$ is the complex conjugate of $\hat{c}_{j,k}$. Thus, in our case the transfer function of p-T with reference p at the j^{th} frequency is calculated according to Eq. (5):

$$G_{T,p}^{p}\left(f_j\right) = \frac{\sum_{k=0}^{N-1} \hat{T}_{j,k}\,\overline{\hat{p}_{j,k}}}{\sum_{k=0}^{N-1} \hat{p}_{j,k}\,\overline{\hat{p}_{j,k}}}. \tag{5}$$

We used the above method to determine the transfer function for several values of N (16, 8, 4, 2, 1). Experience showed that the time-series decomposition and averaging of the different measures greatly reduced the frequency resolution at the relevant low frequency range, thus reducing its selectivity. However, with small N (no, or minimal averaging) the noise of the transfer function was too high. Finally, we concluded that $N = 8$ equal parts with

no overlap ($t \approx 8$ days) is a good compromise. With these numbers the G transfer function seemed to be stable in the low frequency range ($t_{period} \geq$ ~12 h) (Fig. 13) and its coherency $C_{T,p}$ that was calculated according to Eq. (6). seemed to be aligned with it, as it moves in 50-99% range at these low frequencies and drops to 20-40% in case of higher frequencies (Fig. 14).

$$C_{T,p}\left(f_j\right) = \frac{\sum_{k=0}^{N-1} \hat{T}_{j,k}\,\overline{\hat{p}_{j,k}}}{\sqrt{\sum_{k=0}^{N-1} \hat{p}_{j,k}\,\overline{\hat{p}_{j,k}}}\,\sqrt{\sum_{k=0}^{N-1} \hat{p}_{j,k}\,\overline{\hat{p}_{j,k}}}} \tag{6}$$

Self-heating practically effects the equilibrium temperature depending on pressure. It means, the self-heating coefficient can be obtained as the low-frequency limit of the transfer function (temperature response to pressure variations). The amplitude of this limit was estimated to be −1.39 mK/mbar, while the delay of the self-heating effect was previously found to be 5.21 ± 0.7 h.

2.8 Determine the adiabatic effect

Adiabatic events were identified as peaks of the time derivative of the pressure dp/dt. Each candidate event was then inspected on the pressure-temperature diagram and their exact time-bounds were adjusted to match the clearly adiabatic portions of the trajectory. For every event we calculated the Pearson correlation coefficient r between pressure and temperature and the corresponding linear regression slope dT/dp (in mK/mbar). Events with a correlation coefficient $|r| < 0.8$ were discarded. For the remaining events, the mean correlation coefficient was $r = 0.94 \pm 0.018$, and the mean slope was dT/dp = 1.65mK/mbar with 0.25 mK/mbar standard deviation.

We can assume, that this adiabatic effect vanishes after some time, so we can assume that it has no effect on low frequencies with several days long period.

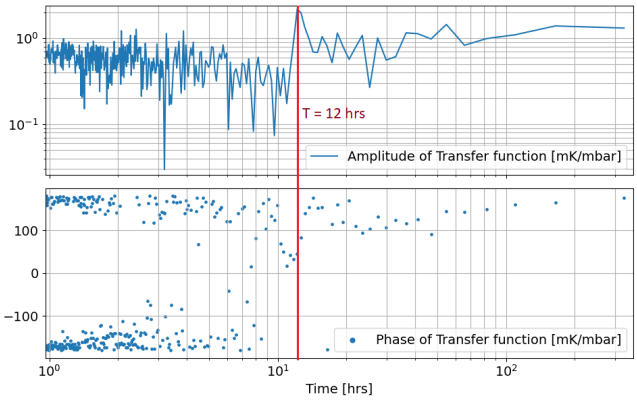

Fig. 13 The amplitude and phase of the calculated transfer function (TF) indicates how temperature residual depends on the atmospheric pressure. X-axis measures the length of period in hours.

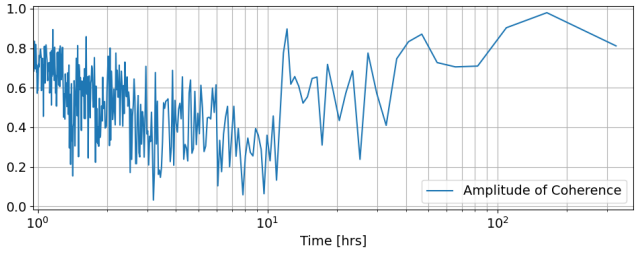

Fig. 14 The coherency of the transfer function is high (50-99%) on low frequencies ($t_{period} \geq$ ~12 h), but drops significantly (to 20-40%) on shorter periods

2.9 Relevant excitation levels

Having established the slope (sensitivity) of the adiabatic temperature change (1.65 mK/mbar) and self-heating (−1.39 mK/mbar - negative sign is obtained from the near 180° phase), as well as the maximum value of the transfer function (2.2 mK/mbar), and taking into account the median sampling interval of the temperature residuals (31–51 min), it can be concluded that excitations with amplitudes below 0.1 mbar, or signals with periods shorter than 1–1.7 h, cannot be considered relevant for the transfer function. These limits can be inferred partly from the coherence function (Fig. 14) and partly from the Fourier spectrum of the pressure signal (Fig. 15).

3 Evaluation of results

The main parameters obtained from the pressure–temperature data analysis, including the adiabatic response, the self-heating component, the characteristic delay, and the relevant time scales of the transfer function are summarised in Table 2.

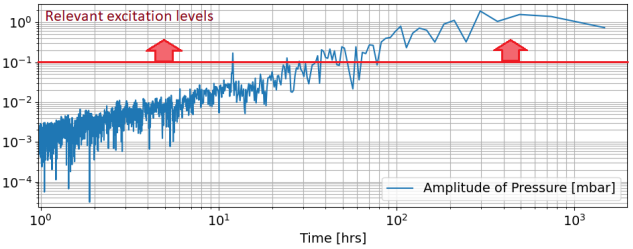

Fig. 15 Amplitude spectrum of the external air pressure as an excitation signal as a function of the period (blue curve). The red line shows the minimum excitation amplitude required for determining the transfer function. It can be clearly seen that relevant excitation took place only for periods of 12 h, 24 h, and above ~36 h.

Table 2 Summary of the main parameters derived from the pressure–temperature analysis. The table lists the characteristic slopes of the adiabatic and self-heating components, the measured delay of the long-term response, the estimated minimum pressure excitation required to generate a detectable temperature change, and the relevant time-scales of the *p-T* transfer function.

Parameter	Description	Estimated value
Adiabatic temperature–pressure slope	Short-term correlated *p-T* response	1.65 ± 0.25 mK/mbar (1σ)
Self-heating coefficient	Long-term anticorrelated *p-T* component	−1.4 mK/mbar
Self-heating delay	Phase delay of long-term component	5.21 ± 0.35 h (1σ)
Minimum effective excitation	Threshold of measurable response	≈ 0.1 bar
Relevant time periods	Significant components in transfer function	12 h, 24 h > 36 h

3.1 Result of compensating the relaxation process

By selecting the appropriate model for the cool-down process (physically meaningful, having minimal standard deviation), the curve and its parameters could be determined with high accuracy. By subtracting this curve three orders of magnitude smaller thermal effects, self-heating of the tiltmeter and adiabatic temperature change could be detected and analysed.

3.2 Physical interpretation of the temperature-pressure dependence

The physical interpretation of the temperature-pressure dependence was successful. Fast pressure changes induce correlated temperature change due to adiabatic process, while slow, long term temperature changes, which were anticorrelated with pressure are identified as self-heating.

3.3 Definition of the *p-T* transfer function

Although the points of the transfer function showed the qualitative properties of the pressure-temperature dependency properly and the values of the predefined model parameters (amplitude and delay) of both effects were determined with high confidence, still we cannot consider the determination of the *p-T* transfer function as a clear success.

The reason is that the original interpretation of 5.21 ± 0.7 h delay cannot be matched to a valid physical model, therefore – using this approach – no matching mathematical model was found.

3.4 Possible enhancements and further steps

Temperature measurement of LTS seems to be limited to the current, improper operation mode. A general, significant enhancement would be to contact the manufacturer, to remove this limitation and have better temperature data in the future.

Another task would be to review the possible physical models of the system, and find a proper mathematical model along with the parameters matching the measurements.

4 Conclusions

In the present study, several conclusions were obtained. First, we concluded that the non-ideal practice of temperature measurement (ignoring quantization rules) can significantly reduce the achievable measurement resolution both in value and time. It causes a drastic limitation on determining the effect of environment.

We also concluded, that slow, but modellable physical processes, such as the natural cool-down of the system, can be separated from other environmental effects when no external excitation or active temperature stabilization is applied. With this approach we can examine effects with intensity several orders of magnitude lower than the long-term transient itself.

Keeping these findings in mind, when performing temperature-sensitive measurements it is advisable to monitor temperature with high resolution and either ensure medium- and long-term stability through active temperature control, or allow the slow thermal transients (e.g., the natural cool-down process) to occur freely. Additionally, it is recommended to apply adequate thermal insulation in order to minimize high-frequency temperature fluctuations originating from active temperature control or transient external influences, such as brief human presence.

However, in case of thermal isolation the so-called self-heating effect of the electrical power used by the instruments must be considered. It means, that during operation it is necessary to ensure the dissipation of heat generated by the instrument. This heat is typically transferred towards a thermally stable, high heat-capacity body, usually the floor using the air as the coupling medium. For the thermal stability the decisive factors are the size of the dissipating surface, i.e., the base area of the thermal enclosure, and the quality of the coupling – namely, whether air can circulate adequately and uniformly between the instrument and the floor.

If pressure under the insulation is not stable, its variations must be considered from two perspectives. First,

sudden pressure changes induce adiabatic temperature variations, the magnitude of which strongly depends on the ratio of the heat capacity of air enclosed beneath the thermal insulation to that of the instrument. The less air present under the insulation, the smaller this effect will be. Second, proper thermal coupling requires sufficient volume for air circulation and sufficient surface area for heat dissipation. Since thermal coupling through air depends on air pressure, reducing pressure dependence of self-heating requires better coupling with larger air volume.

Compared to the traditional, air-based heat transfer it can be more advantageous to employ a metallic connection with high thermal conductivity for the dissipation of self-heat. In this case, there is no need for a larger volume of air under the thermal insulation, so the effect of adiabatic temperature changes can also be minimized by direct insulation of the instrument.

Acknowledgement

The project presented in this article is supported by the HUN-REN Wigner Research Institute for Physics and its colleagues, Péter Ván, Gergely Barnaföldi and Péter Lévai, by providing the underground laboratory, and by the Department of Geodesy and Surveying, Faculty of Civil Engineering at Budapest University of Technology and Economics, especially Lajos Völgyesi and Dr. Gyula Tóth, by providing the LTS tiltmeter and research-related consultation.

References

[1] Eötvös, R., Pekár, D., Fekete, E "Beiträge zum Gesetze der Proportionalität von Trägheit und Gravität" (Contribution to the Law of Proportionality of Inertia and Gravitation), Annalen der Physik, 373(9), pp. 11–66, 1922. (in German) https://doi.org/10.1002/andp.19223730903

[2] Fischbach, E., Sudarsky, D., Szafer, A., Talmadge, C., Aronson, S. H. "Reanalysis of the Eötvös experiment", Physical Review Letters 56, pp 3–6, 1986. https://doi.org/10.1103/PhysRevLett.56.3

[3] Roll, P. G., Krotkov, R., Dicke, R. H. "The equivalence of inertial and passive gravitational mass", Annals of Physics, 26(3), pp. 442–517, 1964. https://doi.org/10.1016/0003-4916(64)90259-3

[4] Braginskii, V. B., Panov, V. L. "Verification of the equivalence of inertial and gravitational mass", Journal of Experimental and Theoretical Physics, 34(3), pp. 463–466, 1972.

[5] Tóth, Gy. "Gravity gradient bias in the EPF experiment", The European Physical Journal Plus, 135(2), 222, 2020. https://doi.org/10.1140/epjp/s13360-020-00242-w

[6] Völgyesi, L., Tóth, G., Szondy, G., Kiss, B., Fenyvesi, E., Barnaföldi, G. G., Égető, C., Lévai, P., Ván, P. "Jelenlegi Eötvös-inga felújítások, fejlesztések és mérések" (Current torsion balance renovations, developments and measurements), Publications in Geomatics, 24, pp. 129–139, 2021. (in Hungarian)

[7] Völgyesi, L., Szondy, G., Tóth, G., Péter, G., Kiss, B., ..., Ván, P. "Preparations for the remeasurement of the Eötvös-experiment", In: International Conference on Precision Physics and Fundamental Physical Constants (FFK2019), Tihany, Hungary, 2019, 041. https://doi.org/10.22323/1.353.0041

[8] Tóth, G., Völgyesi, L., Szondy, G., Péter, G., Kiss, B., ..., Ván, P. "Remeasurement of the Eötvös-experiment, status and first results", In: International Conference on Precision Physics and Fundamental Physical Constants (FFK2019), Tihany, Hungary, 2019, 042. https://doi.org/10.22323/1.353.0042

[9] Völgyesi, L. "Renaissance of Torsion Balance Measurements in Hungary", Periodica Polytechnica Civil Engineering, 59(4), pp. 459–464, 2015. https://doi.org/10.3311/PPci.7990

[10] Völgyesi, L., Tóth, Gy., Szondy, Gy., Kiss, B., Fenyvesi, E., ..., Ván, P. "Report on a pre-earthquake signal detection by enhanced Eötvös torsion balance", [preprint] arXiv, 23 April 2022. https://doi.org/10.48550/arXiv.2202.09607

[11] Perrier, F., Morat, P., Mouël, J.-L. "Pressure induced temperature variations in an underground quarry", Earth and Planetary Science Letters, 191(1–2), pp. 145–156, 2001. https://doi.org/10.1016/S0012-821X(01)00411-3

[12] Perrier, F., Bourges, F., Girault, F., Mouël, J.-L., Genty, D., Lartiges, B., Losno, R., Bonnet, S. "Temperature variations in caves induced by atmospheric pressure variations—Part 1: Transfer functions and their interpretation", Geosystems and Geoenvironment, 2(2), pp. 100–145, 2023. https://doi.org/10.1016/j.geogeo.2022.100145

[13] Widrow, B., Kollar I., Liu, M. C. "Statistical theory of quantization", IEEE Transactions on Instrumentation and Measurement, 45(2), pp. 353–361, 1996. https://doi.org/10.1109/19.492748

[14] Babita, Pant, U., Meena, H., Gupta, G., Bapna, K., Shivagan, D. D. "Evaluation of self-heating effect in platinum resistance thermometers", Measurement, 203, 111994, 2022. https://doi.org/10.1016/j.measurement.2022.111994

[15] Šabacká, P. "Analysis of gas thermal conductivity at low pressures using a mathematical-physical model", Journal of Physics: Conference Series, Brno, Czechia, 2382, 012021, 2022. https://doi.org/10.1088/1742-6596/2382/1/012021

[16] Saidi, M., Abardeh, R. H. "Air pressure dependence of natural-convection heat transfer", In: Proceedings of the World Congress on Engineering, London, UK, 2010, pp. 1444–1447. ISBN 978-988-18210-7-2

[17] Google Maps "Budapest, Wigner Research Centre for Physics", [map] 2025. Available at: https://shorturl.at/UYliz

[18] LGM Lippmann Geophysikalische Messgeräte "Very High Resolution Tiltmeter HRTM - Operating Instructions Version 2.0", [pdf] LGM Lippmann Geophysikalische Messgeräte, Schaufling, Germany, 2017. Available at: https://www.l-gm.de/documents/hrtm_operation_instructions_v2_v1.0.8.pdf

[19] Meurers, B., Papp, G., Ruotsalainen, H., Benedek, J., Leonhardt, R. "Hydrological signals in tilt and gravity residuals at Conrad Observatory (Austria)", Hydrology and Earth System Sciences, 25(1), pp. 217–236, 2021. https://doi.org/10.5194/hess-25-217-2021

[20] Barbély, E., Benedek, J., Leonhardt, R., Horn, N., Szabó, Cs., Molnár, T., Csáki, I., Meurers, B., Papp, G. "A Geodynamic Network for the Monitoring of Seismo–Tectonic Activity Along the Mur–Mürz Fault Line (Austria)", Geophysical Observatory Reports, 2023–2024, pp. 82–105, 2025. https://doi.org/10.55855/gor2024.6

[21] Holman, J. P. "Heat Transfer", McGraw-Hill, 1972. ISBN 978–0–07–352936–3

[22] D'Alessandro, G., de Monte, F. "Multi-Layer Transient Heat Conduction Involving Perfectly-Conducting Solids", Energies, 13(24), 6484, 2020. https://doi.org/10.3390/en13246484